metals

MDPI

Article

Stress Corrosion Cracking in an Extruded Cu-Free Al-Zn-Mg Alloy

Adrian Lervik [1,*], John C. Walmsley [1,2,3], Lars Lodgaard [4], Calin D. Marioara [3], Roy Johnsen [5], Otto Lunder [3], and Randi Holmestad [1]

[1] Department of Physics, Norwegian University of Science and Technology (NTNU), N-7491 Trondheim, Norway; randi.holmestad@ntnu.no (R.H.)
[2] Department of Materials Science and Metallurgy, University of Cambridge, Cambridge CB2 3QZ, UK, jcw80@cam.ac.uk (J.C.W.)
[3] SINTEF Industry, N-7465 Trondheim, Norway; Calin.D.Marioara@sintef.no (C.D.M.); Otto.R.Lunder@sintef.no (O.L.)
[4] Benteler Automotive, 2830 Raufoss, Norway; lars.lodgaard@benteler.com (L.L.)
[5] Department of Mechanical and Industrial Engineering, Norwegian University of Science and Technology, (NTNU), N-7491 Trondheim, Norway; roy.johnsen@ntnu.no (R.J.)
* Correspondence: adrian.lervik@ntnu.no

Abstract: Stress corrosion cracking (SCC) in Cu-free Al-Zn-Mg (7xxx) aluminium alloys limits its use in many applications. In this work, we study in detail the microstructure of a peak and slightly overaged condition in an AA7003 alloy using transmission- and scanning electron microscopy in order to provide a comprehensive understanding of the microstructural features related to SCC. The SCC properties have been assessed using the double cantilever beam method and slow strain rate tensile tests. Grain boundary particles, precipitate free zones, and matrix precipitates have been studied. A difference in the SCC properties is established between the two ageing conditions. The dominating difference is the size and orientation of the hardening phases. Possible explanations correlating the microstructure and SCC properties are discussed.

Keywords: aluminium alloys; stress corrosion cracking; transmission electron microscopy; EBSD; microstructure; grain boundaries

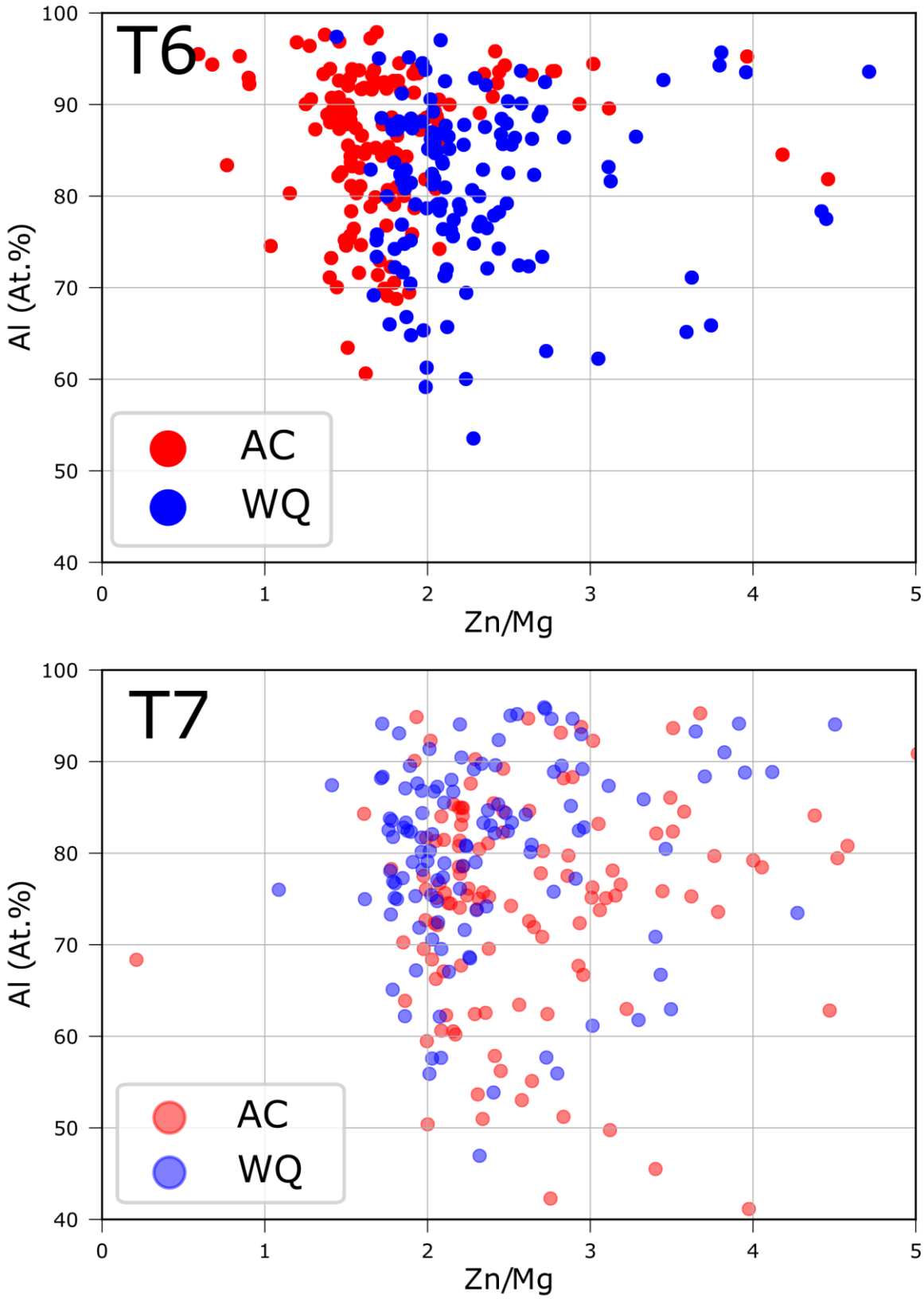

Figure S1. Results from 150 EDS point analysis of grain boundary particles in different tempers acquired using microscope (i) (see main text for details). The Al at.% is shown as function of the Zn/Mg ratio.

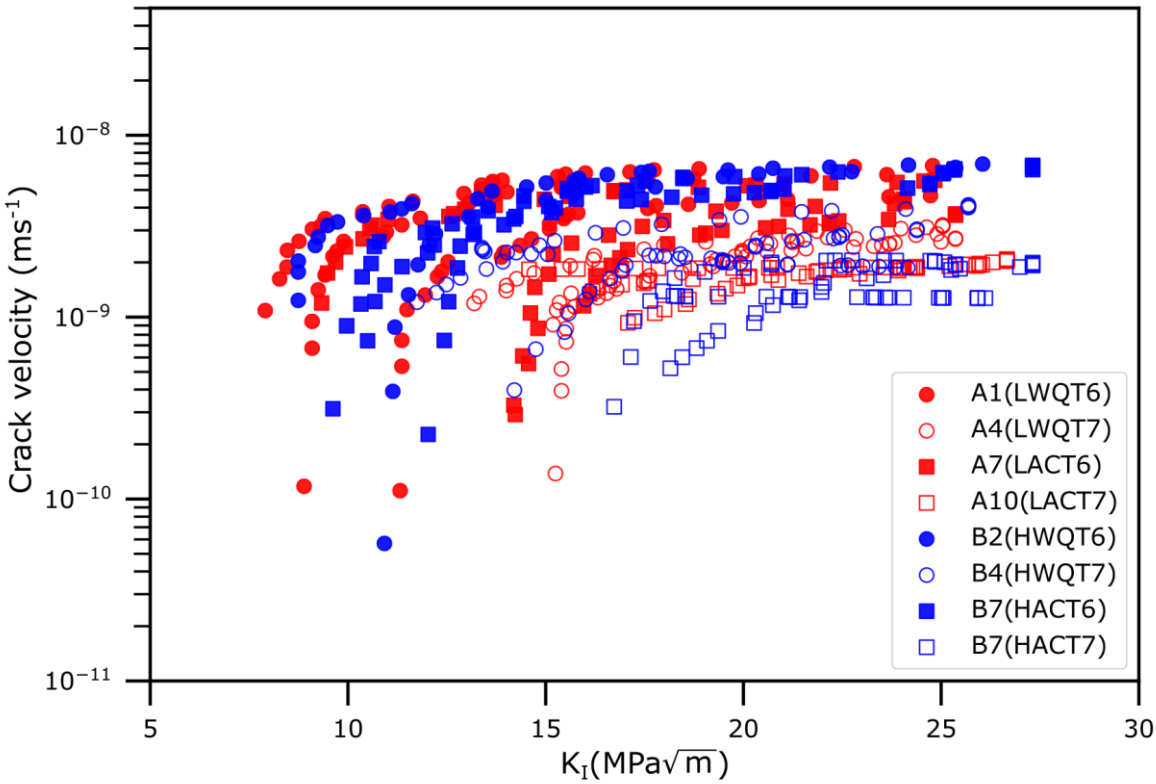

Figure S2. Results from the double cantilever beam tests represented in a conventional crack velocity against stress intensity (K-V) figure.

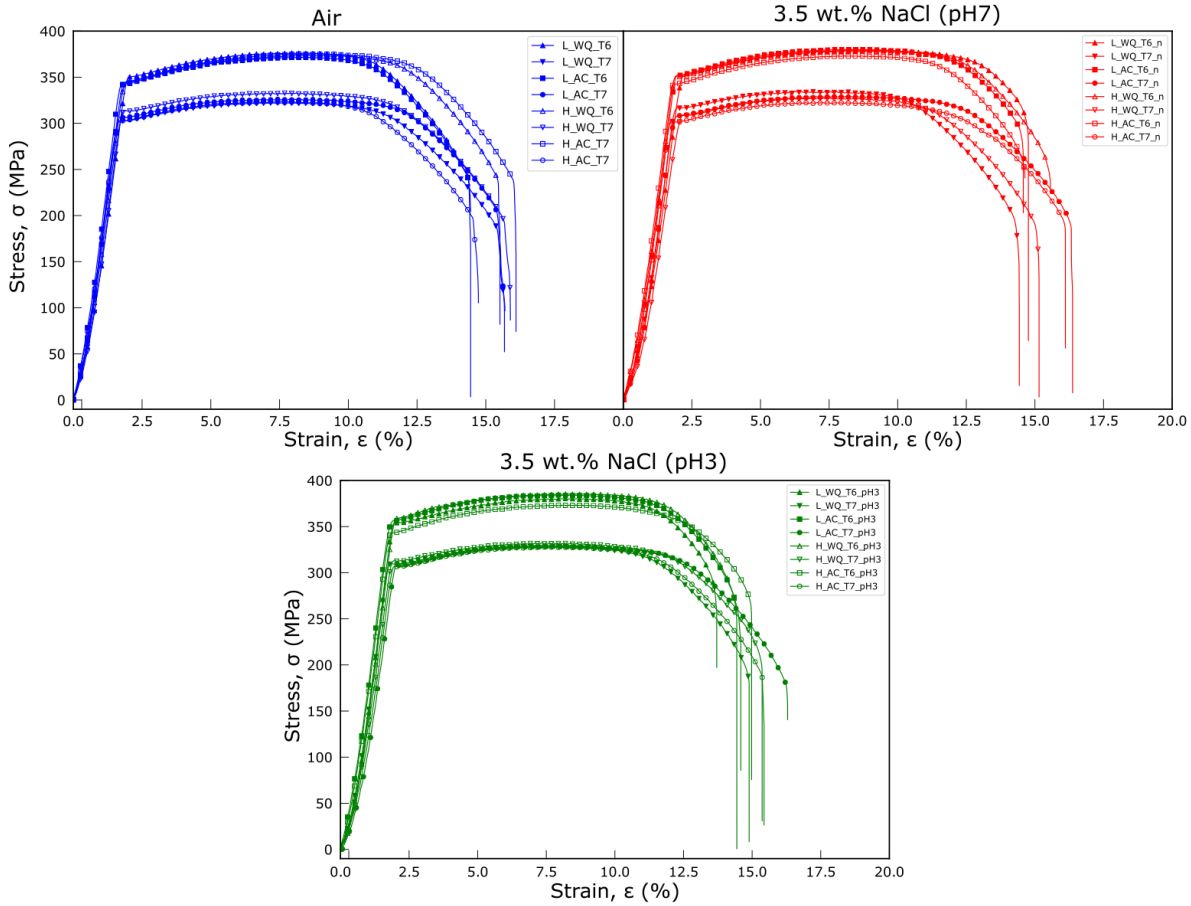

Figure S3. Stress-strain curves for the 4 tempers with two different Si contents, tested in air and 3.5 wt% NaCl solution with different pH.

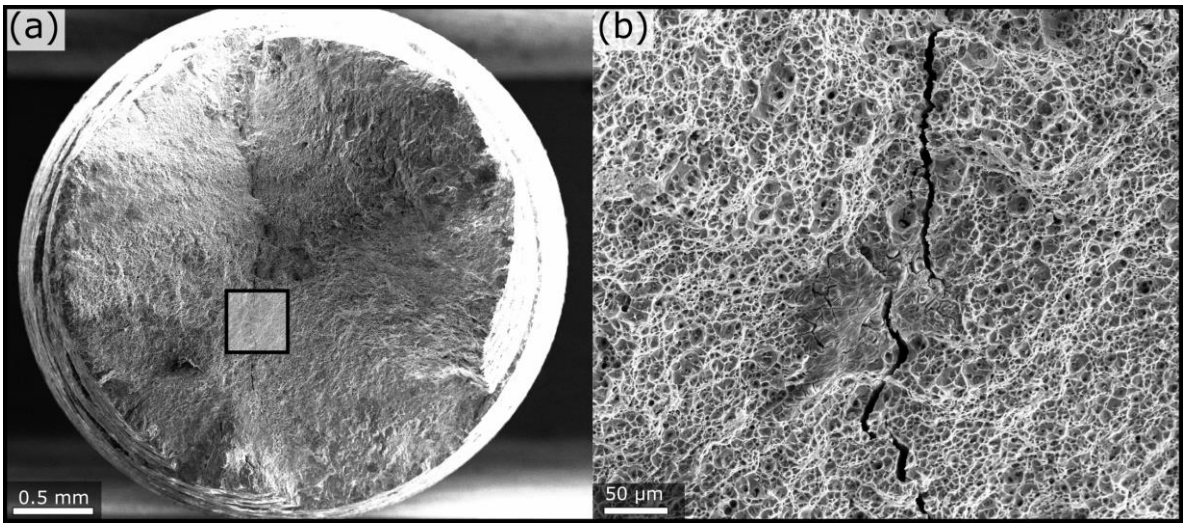

Figure S4. The fracture surface of sample H-AC-T6 (tested in 3.5 wt.% NaCl at pH = 3) imaged using secondary electron (SE)-scanning electron microscopy (SEM), demonstrating a visible crack penetrating through the entire cross-section.

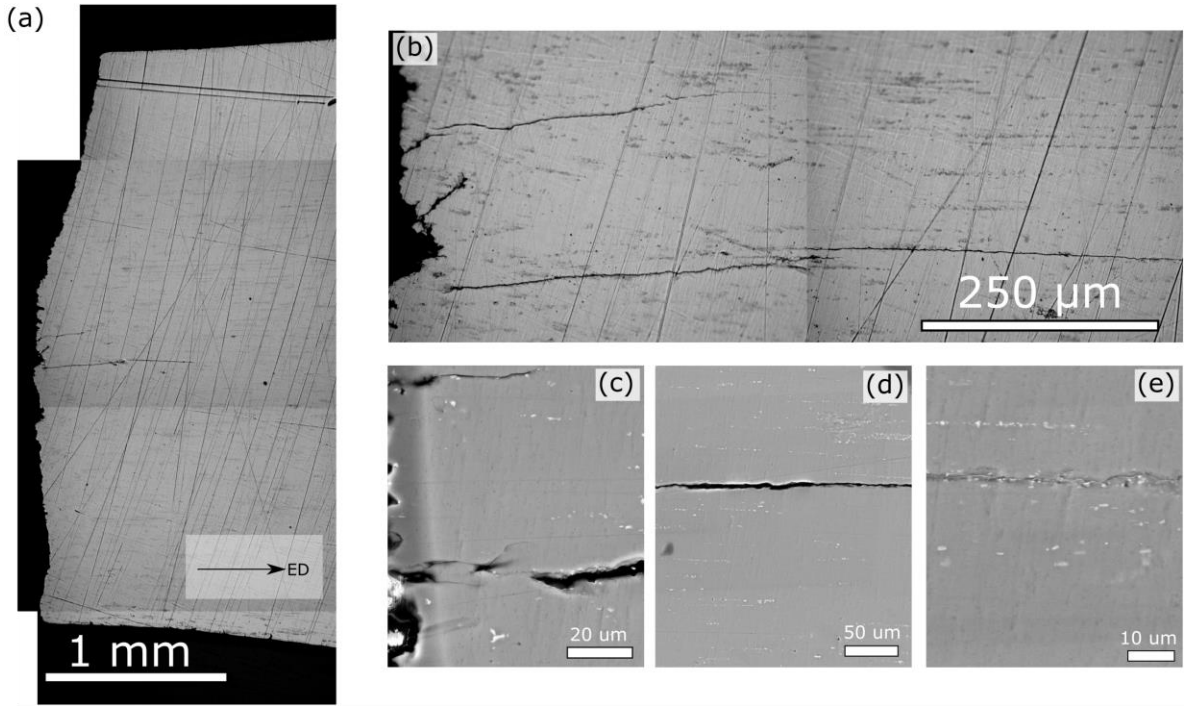

Figure S5. A slow strain rate testing (SSRT) sample embedded in epoxy and polished to reveal the depth extent of the secondary cracks (as in figure A4). Figures (**a**) and (**b**) are optical microscopy images and (**c**)-(**e**) are backscattered electron (BSE)-SEM images.